

## Analysis of local vibrations in the stay cables of an existing cable-stayed bridge under wind gusts

Qingxiong Wu<sup>†</sup>

*College of Civil Engineering, Fuzhou University, No. 2 Xueyuan Road,  
University Town City, Fuzhou, Fujian, China*

Kazuo Takahashi<sup>‡</sup>

*Department of Civil Engineering, Faculty of Engineering, Nagasaki University,  
1-14, Bunkyo-machi, Nagasaki, Japan*

Baochun Chen<sup>†‡</sup>

*College of Civil Engineering, Fuzhou University, No. 2 Xueyuan Road,  
University Town City, Fuzhou, Fujian, China*

*(Received December 28, 2005, Accepted January 8, 2008)*

**Abstract.** This paper examines local vibrations in the stay cables of a cable-stayed bridge subjected to wind gusts. The wind loads, including the self-excited load and the buffeting load, are converted into time-domain values using the rational function approximation and the multidimensional autoregressive process, respectively. The global motion of the girder, which is generated by the wind gusts, is analyzed using the modal analysis method. The local vibration of stay cables is calculated using a model in which an inclined cable is subjected to time-varying displacement at one support under global vibration. This model can consider both forced vibration and parametric vibration. The response characteristics of the local vibrations in the stay cables under wind gusts are described using an existing cable-stayed bridge. The results of the numerical analysis show a significant difference between the combined parametric and forced vibrations and the forced vibration.

**Keywords:** cable-stayed bridge; stay cables; parametric vibration; wind gust response.

---

### 1. Introduction

Stay cables (hereinafter abbreviated to ‘cables’) are important components of cable-stayed bridges. Due to their large flexibility, relatively small mass, and very small structural damping, they often exhibit large-amplitude vibrations. The local dynamic behavior of the cables of a cable-stayed

---

<sup>†</sup> E-mail: wuqingx@fzu.edu.cn

<sup>‡</sup> Ph.D., Corresponding author, E-mail: takahasi@civil.nagasaki-u.ac.jp

<sup>†‡</sup> E-mail: baochunchen@fzu.edu.cn

bridge under dynamic excitation, such as from winds or earthquakes, can easily be compared to that of a harp whose strings have been plucked. Forced vibrations of this kind have been thoroughly analyzed (Abdel-Ghaffar *et al.* 1991, Tuladhar *et al.* 1995, Caetano *et al.* 2000, Caetano *et al.* 2000, Au *et al.* 2001).

Another type of excitation was recognized in the 1980's. It corresponds to the combined forced and parametric vibrations of cables of cable-stayed bridges due to bending vibrations of the girder and/or towers. The coupling between the deflections of the tower and girder and those of the cables at the supports is responsible for the parametric vibration, i.e., the local parametric vibration of cables excited by girder and/or tower oscillations (Uhrig 1993). This is believed to result in some reported oscillations that cannot be reasonably explained by other phenomena (Yoshimura *et al.* 1989).

Generally, if a cable is subjected to axial time-varying displacement at a support due to the global motion of the girder and/or towers, the tension force within the cable changes. When the natural frequency of the global modes in a cable-stayed bridge is close to twice or same as that of the cable, the varying tension force of cables can induce larger-amplitude vibration in the cables. Since multi-cable systems are widely used in cable-stayed bridges, the natural frequencies of the global modes easily become close to the natural frequencies of the stay cables. During vibration tests on the Hitsuishijima cable-stayed bridge (420 m, steel, Japan), the Yohkura Bridge (77 m, timber, Japan), and the Tatura Bridge (890 m, steel, Japan), the local parametric vibrations in some stay cables under excitations in the first some global modes are observed (Fujino *et al.* 1997).

Kovacs was the first to point out the possibility of parametric vibration in cables. Takahashi calculated the instability boundaries of the main instability regions of the simple parametric and combination resonance of a flat-sag cable using the harmonic balance method and the eigenvalue method (Takahashi 1991). Fujino examined the linear and nonlinear internal resonances of the stay cables of a cable-stayed bridge and derived a 3-DOF analytical model for a local cable based on global modes, then performed laboratory tests to check the validity of the approach (Fujino *et al.* 1993, Wanitchai *et al.* 1995). Lilien and Pinto da Costa studied the vibration amplitude caused by parametric excitation of cable-stayed structures and developed non-dimensional analytical formulae that can be applied to any stay cable to calculate threshold amplitudes and limit cycle amplitudes produced by parametric excitation (Lilien *et al.* 1994). Pinto da Costa dealt with the nonlinear vibrations of inclined cables excited by periodic motions of their supports and discussed the nonlinear behaviors of cables (Pinto da Costa *et al.* 1996).

These studies established the instability criteria for the fundamental instability regions. In the studies, the cables were given periodic time-varying displacements. However, the studies did not explain the local vibrations in stay cables of cable-stayed bridges under environmental and service loadings, e.g., wind, earthquakes, and traffic loading, which contain a broad spectrum of excitation frequencies.

This paper uses the in-plane vibration model of stay cables following the idea proposed by Pinto da Costa *et al.* (1996), and the analysis of local vibrations in cables considers the vibration characteristics of an existing steel cable-stayed bridge under sinusoidal excitations, by a moving vehicle or an earthquake. The following conclusions were reached (Wu *et al.* 2001, Wu *et al.* 2003).

- 1) Parametric vibrations of cables in the second unstable region occur under vertical sinusoidal excitation. The amplitudes of cables induced by parametric vibration is of the same order as that induced by forced vibration.
- 2) Parametric vibrations of cables in the principal unstable region appear under torsional

sinusoidal excitation, but only after considerable time has passed.

- 3) The amplitudes of local parametric cable vibrations under excitation by a moving vehicle are small since the amplitude of the girder is small.
- 4) Parametric vibrations in cables do not appear when a moderate ground motion is applied in the longitudinal direction of the bridge.

The other form of excitation related to cable-stayed bridges is wind loading. Stability in wind is an important consideration in the design of cable-stayed bridges, so the parametric vibration of cables under wind loading should be also examined.

In this study, the local vibrations in the cables of an existing cable-stayed bridge under wind gusts are analyzed. A two-step approach is used to study the local vibrations of the stay cables (Wu *et al.* 2001, Wu *et al.* 2003). The global gust vibration of the bridge is investigated first, followed by an examination of the local vibration of the cables.

Local vibration analysis of a cable considers both forced vibration and parametric vibration. In this study, a time domain gust analysis method is used in the analysis of an existing cable-stayed bridge. The time-domain gust approach for cable-stayed bridges considers such time-serial response characteristics as simultaneity and the instantaneous acquisition of the vibration value (Zhu *et al.* 2005). It is difficult to analyze using the frequency domain approach (Jain *et al.* 1996, Xu *et al.* 2000, Boonyapinyo *et al.* 1999). According to Scanlan's theory, gust analysis must consider both the self-excited load and the buffeting load (Scanlan *et al.* 1990, Jain *et al.* 1996, Simiu *et al.* 1996, Ding *et al.* 2000). It is essential, therefore, to convert these two wind loads into time domains using a computer simulation technique. In this paper, the self-excited load is converted using the rational function approximation (Wilde *et al.* 1996, Chen *et al.* 2000), while the buffeting load is converted using the multidimensional autoregressive (AR) process (Iwatani 1982, Iannuzzi *et al.* 1987).

The local vibration of the cable is obtained using a cable that is fixed at one end and has relative time-varying displacements at the other end. The time-varying displacements at the cable supports are obtained from the global vibration.

The properties of local vibration in cables subjected to wind gusts are derived by means of numerical analysis of an existing steel cable-stayed bridge.

## 2. Global vibration analysis due to wind gust

The global response of a bridge in wind gusts is analyzed by defining the coordinate system and aerodynamic forces as shown in Fig. 1. The wind blows lateral to the girder of the bridge and the aerodynamic forces are defined as lift  $L_{ij}$ , drag  $D_{ij}$ , and moment  $M_{ij}$ . Vibration of girder consists of

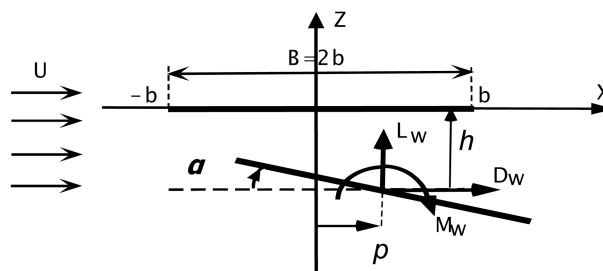


Fig. 1 Wind force and displacement components at a point along bridge axis

vertical displacement  $h$ , horizontal displacement  $p$ , and torsional displacement  $\alpha$ . The wind gust is applied to the girder, and isn't applied to the tower.

### 2.1 Buffeting loads

The buffeting loads per unit span can be expressed based on quasi-steady theory. The steady state wind loads are not considered in the present analysis (Chen *et al.* 2000, Ding *et al.* 2000).

$$\begin{aligned} L_{buf} &= \frac{1}{2}\rho U^2 B \left\{ 2C_L(\alpha_0) \frac{u(x,t)}{U} + \left( C_L'(\alpha_0) + \frac{A}{B} C_D(\alpha_0) \right) \frac{w(x,t)}{U} \right\}, \\ M_{buf} &= \frac{1}{2}\rho U^2 B^2 \left\{ 2C_M(\alpha_0) \frac{u(x,t)}{U} + C_M'(\alpha_0) \frac{w(x,t)}{U} \right\}, \\ D_{buf} &= \frac{1}{2}\rho U^2 B \left\{ 2\frac{A}{B} C_D(\alpha_0) \frac{u(x,t)}{U} \right\} \end{aligned} \quad (1)$$

where  $C_D$ ,  $C_L$  and  $C_M$  are the drag, lift and moment coefficients obtained from wind tunnel tests on a cross-section of a girder model,  $C_L'$  and  $C_M'$  are the slopes of  $C_L$  and  $C_M$ ,  $\alpha_0$  is the effective attack angle of the oncoming wind,  $\rho$  is the air density,  $U$  is the mean wind velocity,  $A$  is the deck height and  $B$  is the deck width.

Fluctuating part  $u(x,t)$  along the wind direction and fluctuating part  $w(x,t)$  in the vertical direction are calculated through simulations using the autoregression (AR) model. The calculations are done in such a manner that the target power spectrum and coherence to the fluctuating wind velocity are satisfied (Iwatani 1982, Iannuzzi *et al.* 1987).

### 2.2 Self-excited loads

The linearized forms of the self-excited force for sinusoidal deflection components  $h(x,t)$ ,  $p(x,t)$ , and  $\alpha(x,t)$  are summarized as follows (Scanlan *et al.* 1990, Jain *et al.* 1996, Simiu *et al.* 1996, Sun 1999, Chen *et al.* 2000).

$$\begin{aligned} L_{se} &= \frac{1}{2}\rho U^2 2B \left( kH_1^* \frac{\dot{h}}{U} - kH_2^* \frac{B\dot{\alpha}}{U} - k^2 H_3^* \alpha + k^2 H_4^* \frac{h}{B} - kH_5^* \frac{\dot{p}}{U} - k^2 H_6^* \frac{p}{B} \right), \\ M_{se} &= \frac{1}{2}\rho U^2 2B^2 \left( -kA_1^* \frac{\dot{h}}{U} + kA_2^* \frac{B\dot{\alpha}}{U} + k^2 A_3^* \alpha - k^2 A_4^* \frac{h}{B} + kA_5^* \frac{\dot{p}}{U} + k^2 A_6^* \frac{p}{B} \right), \\ D_{se} &= \frac{1}{2}\rho U^2 2B \left( kP_1^* \frac{\dot{p}}{U} + kP_2^* \frac{B\dot{\alpha}}{U} + k^2 P_3^* \alpha + k^2 P_4^* \frac{p}{B} - kP_5^* \frac{\dot{h}}{U} - k^2 P_6^* \frac{h}{B} \right) \end{aligned} \quad (2)$$

where  $k = \omega B/U$  is the reduced frequency,  $\omega$  is the natural circular frequency, and  $H_j^*$ ,  $A_j^*$  and  $P_j^*$  are the flutter derivatives of the deck's cross section.

From Eq. (2), it is clear that the self-excited load is dependent not only on wind speed but also on frequency. In order to transform those frequency-dependent loads into frequency-independent loads, Roger proposed a modal method that employs the rational functions of the Laplace variable and introduces 'lag' coefficients that make the resulting frequency-dependent self-excited aerodynamic forces independent of the frequencies by (Rogar 1977). The application of rational function

approximation for flutter and gust analysis of bridges has been the subject of previous studies (Wilde *et al.* 1996, Chen *et al.* 2000).

By applying the rational function to Eq. (2), the self-excited lift  $L_{se}$ , moment  $M_{se}$  and drag  $D_{se}$  on the girder can be expressed as follows.

$$\begin{aligned} \begin{Bmatrix} \frac{L_{se}}{\frac{1}{2}\rho U^2 2B} \\ \frac{M_{se}}{\frac{1}{2}\rho U^2 2B^2} \\ \frac{D_{se}}{\frac{1}{2}\rho U^2 2B} \end{Bmatrix} &= [Q_1] \begin{Bmatrix} h/B \\ \alpha \\ p/B \end{Bmatrix} + \frac{B}{U} [Q_2] \begin{Bmatrix} \dot{h}/B \\ \dot{\alpha} \\ \dot{p}/B \end{Bmatrix} + \sum_{l=1}^N \{\lambda_l\}, \\ \{\lambda_l\} + \frac{U}{B} D_l \{\lambda_l\} &= \frac{U}{B} [Q_{l+2}] \begin{Bmatrix} h/B \\ \alpha \\ p/B \end{Bmatrix} \end{aligned} \quad (3)$$

where  $\{\lambda_l\} = \{\lambda_{1l} \ \lambda_{2l} \ \lambda_{3l}\}^T$  is the vector coefficient of the partial fractions (*lag coefficient*),  $N$  is the number of partial fractions,  $[Q_1]$ ,  $[Q_2]$  and  $[Q_{l+2}]$  are the matrices of the unsteady aerodynamics, and  $D_l$  is a parameter.

If the harmonic vibration is assumed, the rational functions in the frequency domain can be deduced as follows

$$\begin{aligned} \begin{Bmatrix} \frac{L_{se}}{\frac{1}{2}\rho U^2 2B} \\ \frac{M_{se}}{\frac{1}{2}\rho U^2 2B^2} \\ \frac{D_{se}}{\frac{1}{2}\rho U^2 2B} \end{Bmatrix}^T &= [\bar{Q}\{ik\}] \begin{Bmatrix} h/B \\ \alpha \\ p/B \end{Bmatrix} \\ [\bar{Q}\{ik\}] &= [Q_1] + [Q_2] \cdot (ik) + \sum_{l=1}^m \frac{[Q_{l+2}]}{ik + D_l} \end{aligned} \quad (4)$$

By using non-dimensional flutter derivatives ( $H_j^*$ ,  $A_j^*$  and  $P_j^*$ ), which are obtained through wind tunnel tests on a deck's cross-section, the matrix  $[Q(ik)]$  can be expressed as follows.

$$[Q(ik)] = \begin{bmatrix} 2k^2 H_4^* + i2k^2 H_1^* & -k^2 H_3^* - ik^2 H_2^* & -2k^2 H_6^* - i2k^2 H_5^* \\ -k^2 A_4^* - ik^2 A_1^* & \frac{1}{2}k^2 A_3^* + i\frac{1}{2}k^2 A_2^* & k^2 A_6^* + ik^2 A_5^* \\ -2k^2 P_6^* - i2k^2 P_5^* & k^2 P_3^* + ik^2 P_2^* & 2k^2 P_4^* + i2k^2 P_1^* \end{bmatrix} \quad (5)$$

Comparing the coefficients of matrix  $[Q(ik)]$  with  $[\bar{Q}(ik)]$  yields the parameters in  $[\bar{Q}(ik)]$ .

Since the relationship between  $D_l$  and  $Q_l$  is nonlinear, nonlinear optimization must be employed. Applying linear and nonlinear multilevel optimizations in the least-squares rational function approximation formula simultaneously computes and optimizes the unknown coefficients  $[Q_1]$ ,  $[Q_2]$ ,  $[Q_{l+2}]$  and  $D_l$  (Gill *et al.* 1972). The value of nonlinear parameter  $J$ , which is expressed as Equation (6), is set so as to reduce the total approximation error.

$$J = \sqrt{\sum_i \sum_j w_{ij} \varepsilon_{ij}(D_1, D_2, \dots)}, \quad (6)$$

where  $w_{ij}$  is the weighting factor,  $\varepsilon_{ij} = \sum_n \|\bar{Q}_{ij}(ik_n) - Q_{ij}(ik_n)\|^2$ , and  $k_n$  is the  $n$ -th set of reduced frequency for which tabular data are available.

### 2.3 Gust response

The equations of motion for a bridge structural system under wind loads can be expressed as follows.

$$[M]\{\ddot{y}\} + [C]\{\dot{y}\} + [K]\{y\} = \{F\} \quad (7)$$

where  $[M]$  is the mass matrix,  $[C]$  is the damping matrix,  $[K]$  is the stiffness matrix,  $\{F\} = \{F_{se}\} + \{F_{buf}\}$  is the load vector that consists of buffeting wind loads  $\{F_{buf}\}$  and self-excited wind loads  $\{F_{se}\}$ ,  $\{y\}$  is the displacement vector representing the displaced shape of the bridge,  $\{\dot{y}\}$  is the velocity vector and  $\{\ddot{y}\}$  is the acceleration vector.

The modal analysis approach is used to compute the state space equation of the extension system expressing the gust response. Subsequently, the global response of the girder under wind gust is obtained by solving Eq. (7) using the Runge-Kutta method.

## 3. Local vibration analysis of cables considering parametric vibration

An in-plane model of an inclined cable on a cable-stayed bridge is shown in Fig. 2. The cable in this model is fixed at one end and has time-varying displacements  $(X(t), Y(t))$  at the other end. Because the bridge deck and the tower vibrate simultaneously, the displacements  $X(t)$  and  $Y(t)$  are relative components, not absolute components.

The main girder and the main tower are vibrated in the three dimensions, and then the stay cables are also vibrated in the in-plane and out-of-plane direction. The present study focuses the in-plane vibration of stay cables, in which the axial force of cable is supremacy, and ignores the out-of-plane vibration of stay cables. Therefore, the following are assumed for the local vibration analysis of the cables under wind gust.

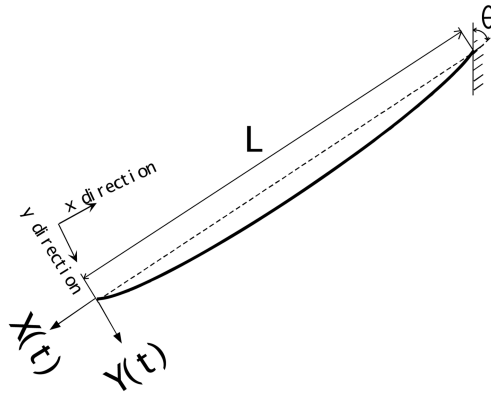


Fig. 2 Geometry of Stay-cable and its boundary conditions

- (1) The first modes of the cables are considered in the analysis.
  - (2) The effect of dampers installed on the cables is omitted.
  - (3) The quasi-steady theory is used to deal with the aerodynamic damping of the cables subjected to wind. The gust response of the cables for both the global buffeting vibrations of the whole bridge and the local vibrations of the stay cables is neglected.
  - (4) Lateral (out-of-plane and coupled in-plane and out-of-plane) vibrations are not considered.
- The equation of motion for a flat-sag cable is given below (Wu *et al.* 2001, Wu *et al.* 2003).

$$m \frac{\partial^2 v_c}{\partial t^2} - P \frac{\partial^2 v_c}{\partial x^2} - \Delta P \left( \frac{\partial^2 v_c}{\partial x^2} + \frac{\partial^2 v_0}{\partial x^2} \right) = 0, \quad (8)$$

$$\Delta P = \frac{EA_c}{L} \left\{ u_c|_{x=L} - u_c|_{x=0} + \frac{1}{2} \int_0^L \left( \frac{\partial v_c}{\partial x} \right)^2 dx + \int_0^L \left( \frac{\partial v_c}{\partial x} \cdot \frac{\partial v_0}{\partial x} \right) dx \right\}$$

where  $u_c$  and  $v_c$  are the displacements in the axial direction ( $x$  direction) and in the normal direction ( $y$  direction) of the cable (see Fig. 2),  $m$  is the mass per unit length of the cable,  $P$  is the initial tension of the cable,  $\Delta P$  is the additional tension produced by local vibration in the cable,  $v_0 = mg/2P(-x^2 + Lx)$  is the initial shape of the cable,  $E$  is the Young's modulus of the cable,  $A_c$  is the cross sectional area of the cable,  $L$  is the span of the cable,  $g$  is the gravitational acceleration and  $t$  is the time.

The following equation describes the assumed responses  $u_c(x,t)$  and  $v_c(x,t)$  of the cable, which at one support receives displacement component  $X(t)$  in the  $x$  direction and displacement component  $Y(t)$  in the  $y$  direction.

$$u_c(x,t) = \left(1 - \frac{x}{L}\right)X(t), \quad v_c(x,t) = \left(1 - \frac{x}{L}\right)Y(t) + \sum_{i=1}^{\infty} T_i(t) \sin \frac{i\pi x}{L}, \quad (9)$$

where  $T_i(t)$  is the time function of the  $i$ -th mode of the cable.

Inserting Eq. (9) into Eq. (8) yields a nonlinear equation of motion of the cable. Applying a Galerkin method produces the following nonlinear equation of motion, which considers both structural damping and aerodynamic damping.

$$\ddot{T}_1(t) + \left(2\omega_1 h_c + \frac{\rho U A_c C_D^C}{2m}\right) \dot{T}_1(t) + \omega_1^2 T_1(t) + B_1(t)T_1(t) + B_2 T_1^2 + B_3 T_1^3 = B_4(t) \quad (10)$$

where  $B_1(t) = \omega_0^2 \left( \frac{X(t)}{X_0} + \frac{1}{2L} \cdot \frac{Y^2(t)}{X_0} - \frac{LA_1}{2} \cdot \frac{Y(t)}{X_0} \right)$ ,  $B_2 = -\omega_0^2 \frac{3LA_1}{\pi} \cdot \frac{1}{X_0}$ ,  $B_3 = +\omega_0^2 \frac{\pi^2}{4L} \cdot \frac{1}{X_0}$ ,  $B_4(t) = \omega_0^2$

$\left\{ -\frac{2}{\pi\omega_0^2} \cdot \ddot{Y}(t) + \frac{2}{\pi\omega_0^2} \cdot \frac{\rho U A_c C_D^C}{2m} \dot{Y}(t) + \frac{4L^2 A_1}{\pi^3} \cdot \frac{X(t)}{X_0} + \frac{2LA_1}{\pi^3} \cdot \frac{Y^2(t)}{X_0} - \frac{2L^3 A_1^2}{\pi^3} \cdot \frac{Y(t)}{X_0} \right\}$ ,  $X_0 = \frac{PL}{EA}$ ,  $A_1 = \frac{mg \sin \theta}{P}$ ,

$\omega_0 = \frac{\pi}{L} \sqrt{\frac{P}{m}}$  is the natural circular frequency of the string with no sag,  $\omega_1 = \frac{\pi}{L} \sqrt{\frac{P}{m} \cdot \left(1 + \frac{8L^3 A_1^2}{\pi^4} \cdot \frac{1}{X_0}\right)}$

is the natural circular frequency of the cable considering sag,  $h_c$  is the damping constant,  $\theta$  is the inclined angle, and  $C_D^C$  is the coefficient of drag force.

The response of the cable is obtained by numerical integration of equation (10) using the Runge-Kutta method.

**4. Global gust response of studied bridge**

Oshima Bridge is a steel cable-stayed bridge in Nagasaki, Japan. The main span of this bridge is 350.0 m and the side spans are 160.0 m. The towers are A-shaped, and the cables are a two-plane, multiple system (Wu *et al.* 2001, Wu *et al.* 2003). A general layout of the bridge and the numbering of the cables are shown in Fig. 3. The girder in the three-dimensional FE model is a single central

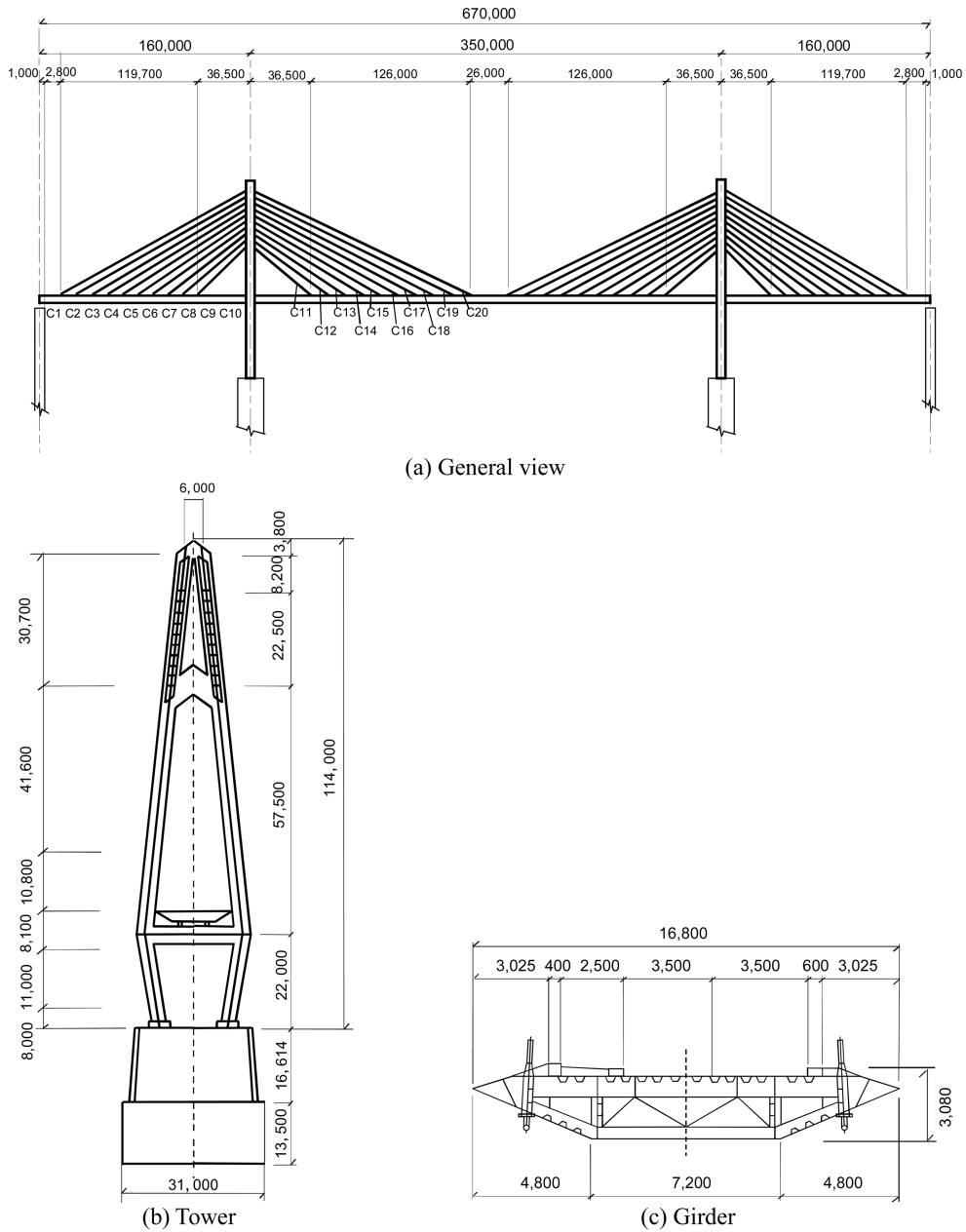


Fig. 3 General view of the cable-stayed bridge (unit: mm)

spine with offset links to the cable anchor points. The towers and piers are modeled using three-dimensional linear beam elements based on the cross-section properties of actual towers and piers. The cables are modeled as linear truss elements with initial tension. The nonlinear behavior of the cables due to their sags is taken into account by using an equivalent modulus of elasticity (Gimsing 1997). Regarding the boundary conditions, the girder is free to move in the longitudinal direction and restrained at the supports in the vertical and transverse directions. Only the rotational component around the longitudinal axis is restrained. The tower bases are restrained in all degrees of freedom. The logarithmic decrement of modal damping of the bridge is 0.02 and the time interval of numerical integration is 0.05s.

Because each cable is represented by a single truss element, the FE model is called an OECS model (One-Element-Cable System) (Abdel-Ghaffar *et al.* 1991). The natural frequencies of the global modes obtained using a MECS model (Multi-Element-Cable System) differ by no more than 1.0% from those obtained using the OECS model (Wu *et al.* 2003). About this bridge used in this paper, the multi-cable system is adopted and this girder is steel, then the weights of cables are slight and the force of cables are relatively slow. So the influence of cable vibrations on global vibrations is extremely small. At the same time, the excitations are environmental or service loadings, not the severe excitations used in (Caetano *et al.* 2000). Therefore, focused on this bridge, this indicates that the local cable vibration can be separated from the deck-tower-cable global vibration.

The natural frequencies of the single cable model obtained from the Irvine equation (Irvine 1981), in which the cables are fixed at the supports, agree well with those obtained from the MECS model. Therefore, it can be concluded that the separation of cable vibrations from the global vibration is valid in the present cable-stayed bridge. Some of the main natural modes obtained from the OECS model are shown in Fig. 4.

The global vibration analysis in this study takes into account the aerodynamic forces of the girder. The static drag, lift, and moment coefficients of a typical deck on this bridge are listed in Table 1.

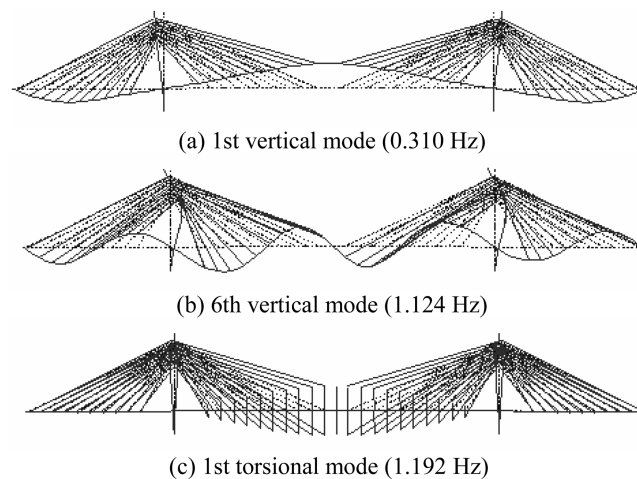


Fig. 4 Modal shapes of the global vibration

Table 1 Aerodynamic coefficients ( $\alpha=0$ )

$C_D = 0.85$ ,	$C_L = 0.19$ ,	$C_M = 0.01$
$C'_D = 0.00$ ,	$C'_L = 3.42$ ,	$C'_M = 1.00$

Although it was originally desirable to obtain the self-excited coefficients  $H_j^*$  and  $A_j^*$  through testing, the present study employs the aerofoil case coefficients. The self-excited coefficients,  $P_j^*$ , which concern the horizontal vibration, are evaluated using quasi-steady theory, and the aerodynamic lift and the pitching moment with the horizontal vibration are neglected. The turbulence spectra are defined as the von Karman spectrum (Panofsky 1984), in the longitudinal direction

$$\frac{fS_u(f)}{\sigma_u^2} = \frac{4n_u}{(1 + 70.8n_u^2)^{5/6}}, \quad n_u = \frac{fL_u^x}{U} \quad (11)$$

and in the vertical direction

$$\frac{fS_w(f)}{\sigma_w^2} = \frac{4n_w(1 + 755.2n_w^2)}{(1 + 283.2n_w^2)^{11/6}}, \quad n_w = \frac{fL_w^x}{U} \quad (12)$$

The atmospheric coherence is set using the exponential estimation by Davenport (Davenport 1961).

$$COH_D(\Delta L, f) = \exp\left\{-K\frac{f\Delta L}{U}\right\} \quad (13)$$

where  $L_u^x = 80$  m,  $L_w^x = 40$  m,  $\sigma_u = I_u U$ ,  $\sigma_w = I_w U$ ,  $I_u = 0.10$ ,  $I_w = 0.05$ ,  $K$  is the coherence decaying coefficient,  $\Delta L$  is the distance between two generated spots, and  $f$  is the frequency. The coherence-decaying coefficient is assumed to be 8.0 for both the longitudinal and transverse velocity components.

Using the AR model to simulate a fluctuating wind, the frequency domain of the power spectrum being considered ranges from 0.05 Hz to 5.0 Hz. The total time is 1200s with a time interval of 0.1s.

Regarding the rational functions approximation, matrices  $[Q_1]$ ,  $[Q_2]$ ,  $[Q_{2+1}]$  and  $[Q_{2+2}]$ , and parameters  $D_1$  and  $D_2$  are quantified as follows with the number of partial fractions  $N$  is assumed to be 2.

$$\begin{aligned} [Q_1] &= \begin{bmatrix} -1.51937 & 3.53404 & 0.00000 \\ -0.37984 & 0.88351 & 0.00000 \\ 0.00000 & 0.00000 & 0.00000 \end{bmatrix}, & [Q_2] &= \begin{bmatrix} -6.29742 & 4.71238 & -0.76000 \\ -1.57435 & -0.39270 & -0.04000 \\ 0.38000 & 0.09500 & -3.40000 \end{bmatrix}, \\ [Q_{2+1}] &= \begin{bmatrix} -0.04133 & 0.20837 & 0.00000 \\ -0.01033 & 0.05209 & 0.00000 \\ 0.00000 & 0.00000 & 0.00000 \end{bmatrix}, & D_1 &= 0.1207, \\ [Q_{2+2}] &= \begin{bmatrix} 0.55044 & 0.37676 & 0.00000 \\ 0.13761 & 0.09419 & 0.00000 \\ 0.00000 & 0.00000 & 0.00000 \end{bmatrix}, & D_2 &= 0.4842 \end{aligned}$$

Fig. 5 shows the results of per-  $2 \times 2$  term, both tabular values and approximate values, with the reduced wind velocity as a parameter. This approximation function provides sufficient precision in all cases. Fig. 6 reflects a fluctuating wind  $u(t)$ ,  $w(t)$  and power spectra of the middle of the main span. The power spectra of the approximate values match well with those of the tabular values.

Fig. 7 shows the r.m.s responses at the middle of the main span in time domains and frequency domains at wind speeds of  $U = 30, 40, 50$ , and  $52$  m/s.  $52$  m/s is the design wind speed for the girder of this bridge. The first 100 natural modes of this bridge (about up to 10 Hz) are considered. The gust analysis in the frequency domain takes into account the modal coupling (Scanlan 1988),

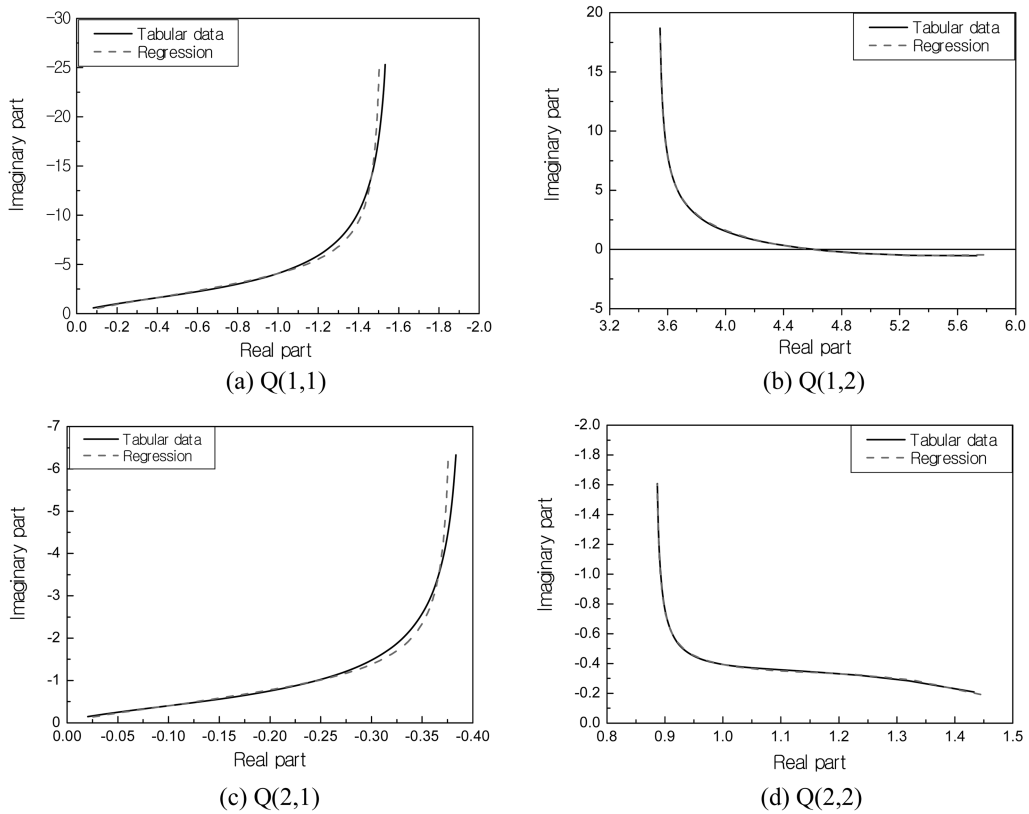


Fig. 5 Approximation using rational functions

which is proposed by Chen *et al.* (2000). The validity of the global gust response analysis is confirmed by the good agreement of these two methods.

### 5. Local vibration characteristics of cables under turbulent wind

The local cable vibration is analyzed using the calculated responses of the girder and towers. The responses of the girder at the fixed point for the left cable are not the same as those at the fixed point for the right cable, since the torsional and vertical gust responses are included in the response analysis of the girder. Therefore, 20 cables on each side of the girder are analyzed. The cables are numbered sequentially from the side span to the main span. The cables on the left side are labeled C1~C20, and the cables on the right side are labeled C21~C40. Since the bridge is symmetric, the cables on the left side (see Fig. 3) are used for the numerical calculations.

#### 5.1 Global modes and local modes

Fig. 8 demonstrates the relationship between the natural frequencies of the global modes and the cables. This figure shows the first natural frequencies of the cables (corresponding to the second unstable region), the natural frequencies multiplied by 2 (corresponding to the principal unstable

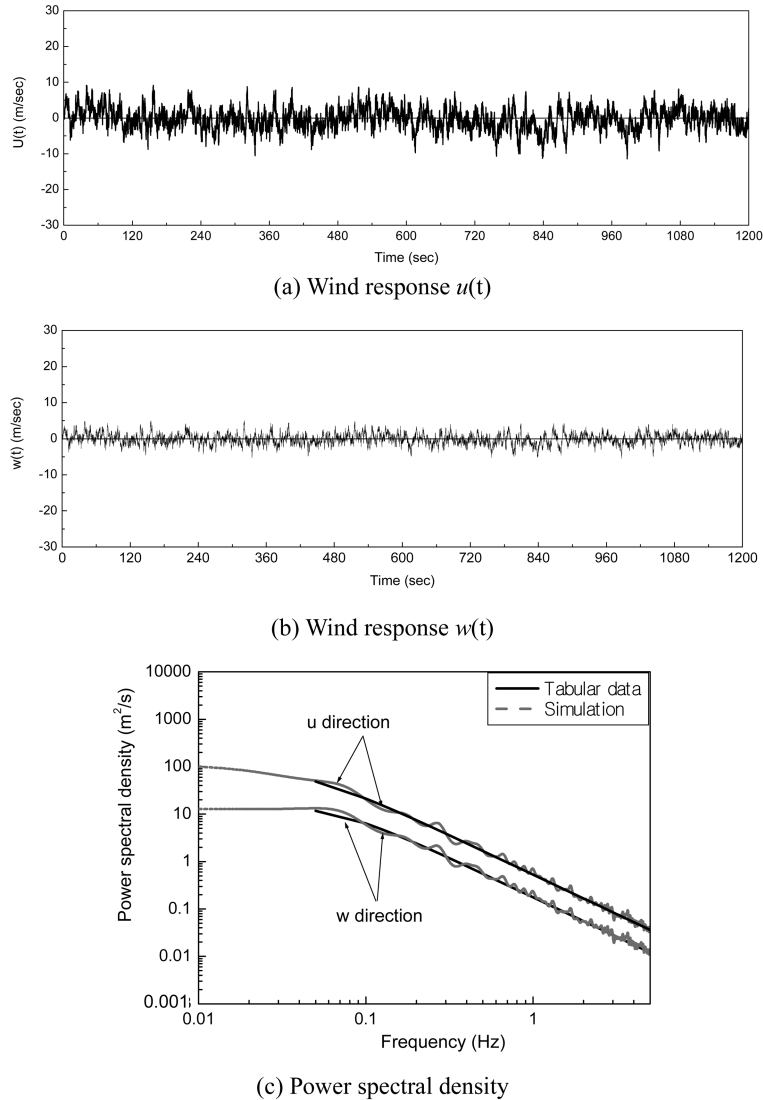


Fig. 6 A fluctuating wind loads  $u(t)$ ,  $w(t)$  and power spectrum of the middle of main span ( $U = 30$  m/s)

region), and the natural frequency divided by 2 (corresponding to the second super-harmonic resonance region).

Since the natural frequency of the 3rd vertical mode of vibration is close to the first natural frequencies of cables C18 (C38) (values in parenthesis are for the cable on the right side), the local parametric vibration in the second unstable region in these cables may occur. According to this figure, the cables in which local nonlinear vibration may occur are listed in Table 2.

## 5.2 Local cables characteristics

Fig. 9 shows the maximum responses of all cables and the girder at the fixed points of the cables under

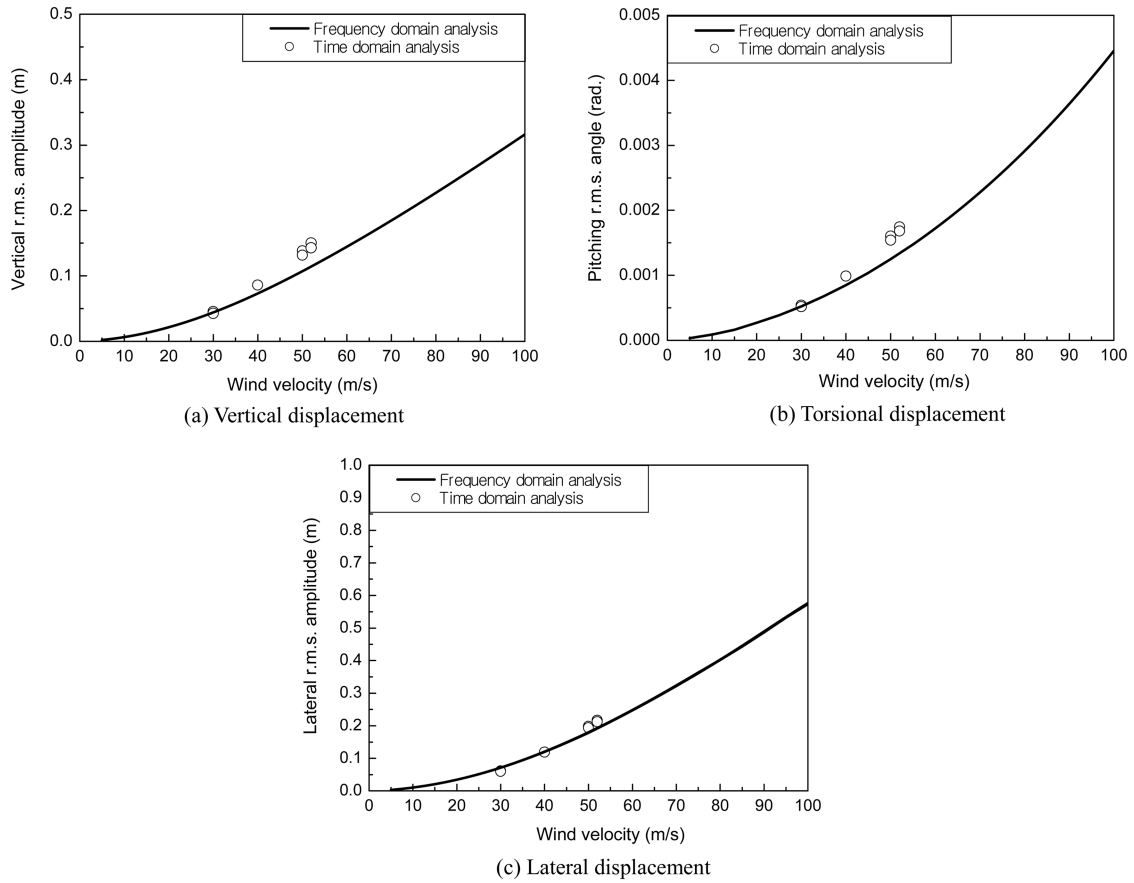


Fig. 7 r.m.s value of vertical, torsional and lateral displacements of the middle of main span

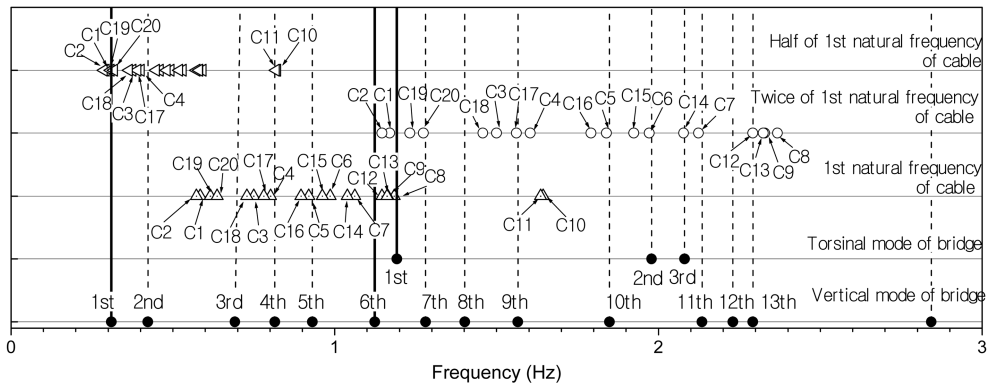


Fig. 8 Relationship between natural frequencies of global modes and natural frequencies of cables

a wind with a velocity of  $U = 30$  m/s. The damping constants  $h_c$  of the cables are assumed to be 0.001.

The maximum responses of cables C12 (C32) and C19 (C39) are seen to be greater than those of the other cables. Fig. 9(c) shows that the ratio of the maximum response of cable C32 to that of the

Table 2 Cables in which local parametric vibration may occur

Global Mode	Frequency (Hz)	Local cable vibration		
		Second unstable region	Principle unstable region	Second super-harmonic resonance region
1st vertical mode	0.310	---	---	C1, C2, C19, C20 (C21,C22,C39,C40)*
2nd vertical mode	0.423	---	---	---
3rd vertical mode	0.692	C18, C19, C20 (C38, C39, C40)	---	C10, C11 (C20, C21)*
4th vertical mode	0.815	C4, C17 (C34, C37)	---	---
5th vertical mode	0.931	C5, C15 (C25, C35)	---	---
6th vertical mode	1.124	C12 (C32)	C2 (C22)	---
1st torsional mode	1.192	C8, C9 (C28, C29)	C1 (C21)	---

\*Figs in parenthesis are the cables on the right side.

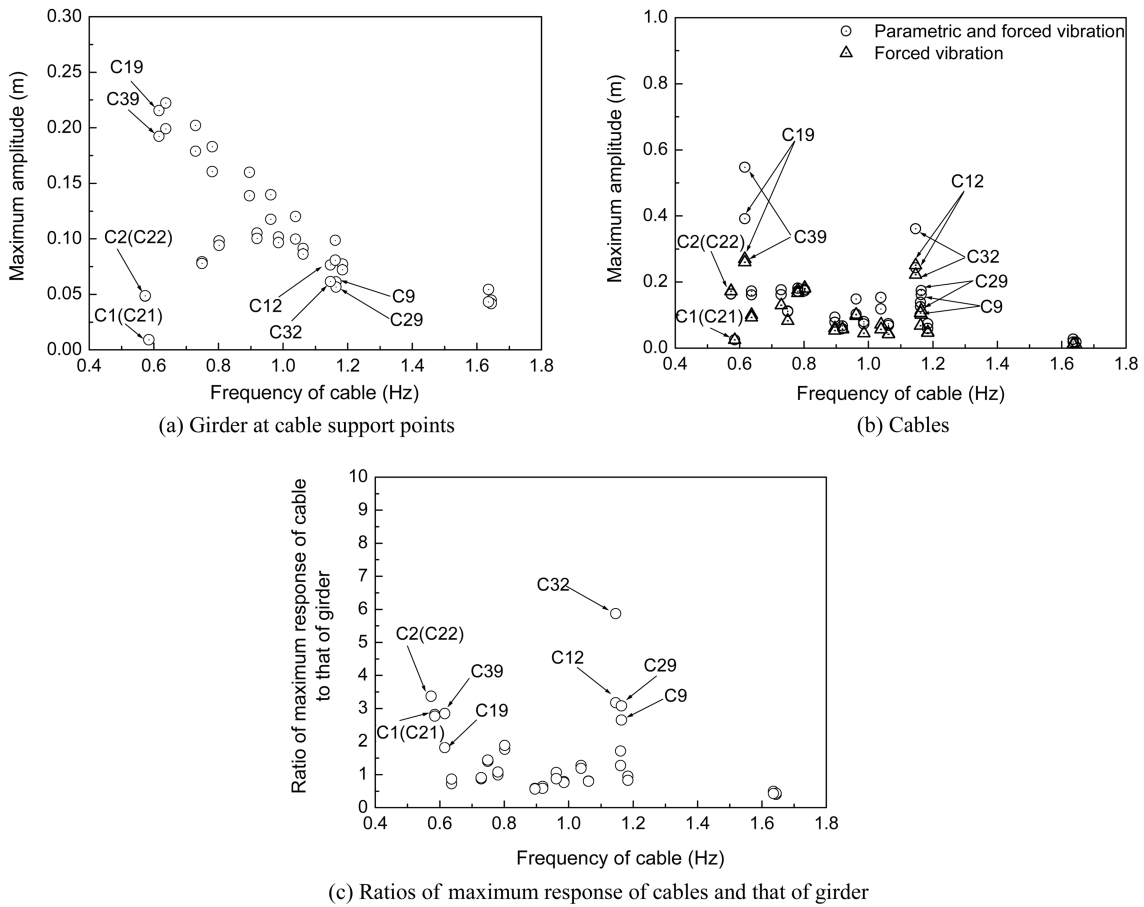


Fig. 9 Maximum responses of the girder and the cables ( $U = 30$  m/s,  $h_c = 0.001$ )

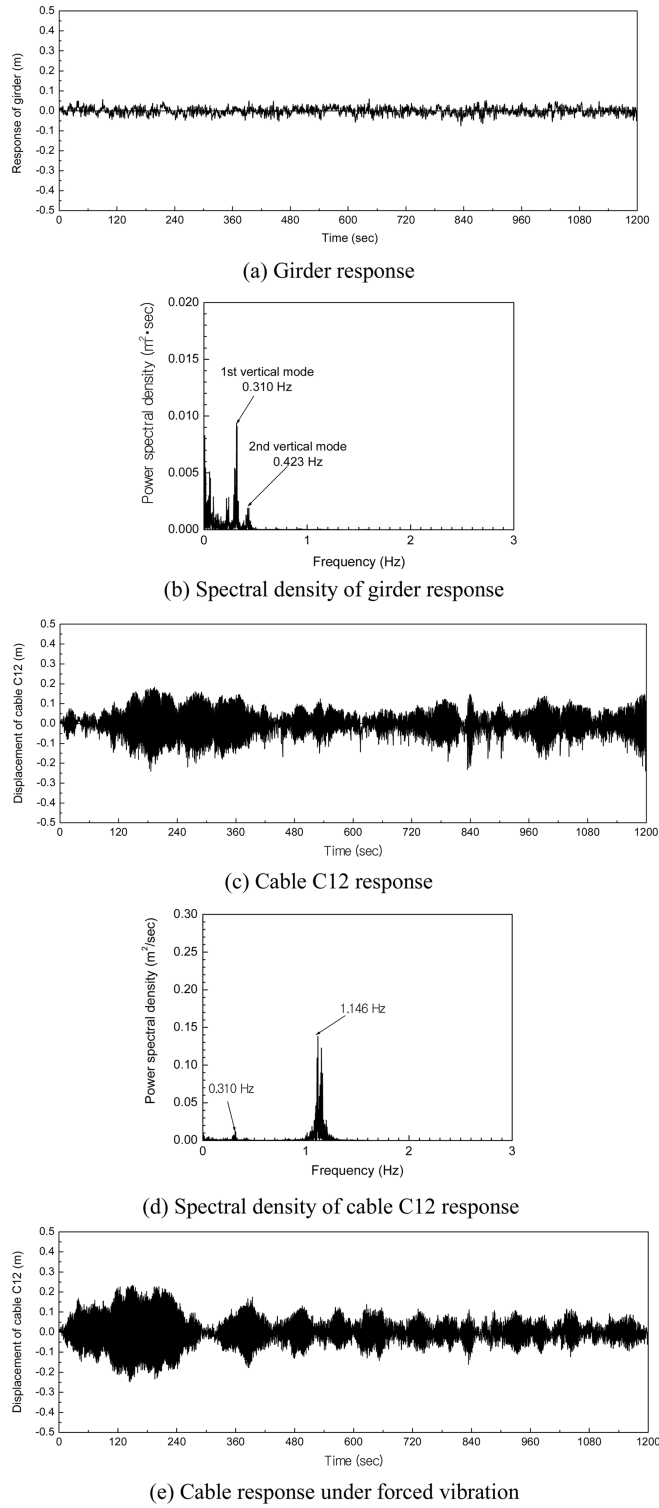


Fig. 10 Response of the girder and cable C12 ( $U = 30 \text{ m/s}$ ,  $h_c = 0.001$ )

girder is around 6.

Since the torsional and vertical gust responses at the fixed points of the cables are included (refer to Eq. (14)), the responses of cables C12 and C32, and cables C19 and C39 differ, even though they have the same natural frequencies.

### 5.2.1 Parametric and/or forced vibrations in Cables C12 and C32

The response properties of Cables C12 and C32 are discussed first. The time responses and spectra of the girder and cables C12 are shown in Fig. 10.

The predominant frequencies of the girder response are about 0.310 Hz and 0.423 Hz, while those of cable C12 are 0.310 Hz and 1.146 Hz. It is necessary to examine the reason why the vibrations of cables C12 and C32 become great even when the 6<sup>th</sup> vertical mode (1.124 Hz) is not predominant, as can be seen in Table 2.

The response of the cable may include components of the parametric vibrations and nonlinear forced vibration with harmonic resonance, super-harmonic resonance or sub-harmonic resonance. These are attributed to the nonlinear equation of motion for the cable, i.e. Eq. (10). In other words, the properties of a cable cannot be distinguished because the response of the cable includes components of both parametric vibration and forced vibration. Therefore, in order to determine the response characteristics of cables C12 and C32, it is essential to distinguish the component of parametric vibration from that of forced vibration.

This problem is solved by analyzing the response of the cable and neglecting the component of parametric vibration  $B_1(t)$  in Eq. (10). The maximum responses of cables C12 and C32 under forced vibration are listed in Table 3.

Since the maximum amplitude of cable C12 under forced vibration is close to that of the cable under the combined effect of parametric and forced vibrations, it can be concluded that the influence of parametric vibration in C12 is small while that of forced vibration is great.

Parametric vibration in the secondary unstable region in cable C32 occurs because the maximum amplitude under parametric and forced vibrations is almost twice greater than the maximum amplitude under forced vibration.

### 5.2.2 Second super-harmonic resonance in cables C19 and C39

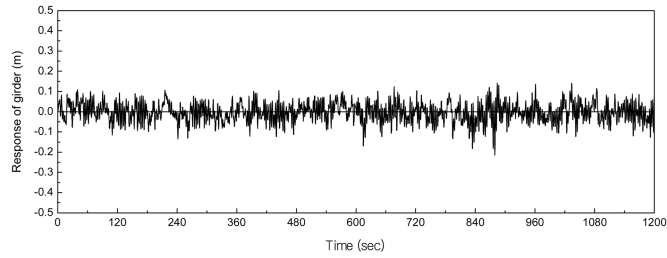
The characteristics of cables C19 and C39 are discussed herein. As shown in Table 4, the vibration in cables C19 and C39 is generated under the combined effect of parametric and forced

Table 3 Maximum responses of cables C12 and C32

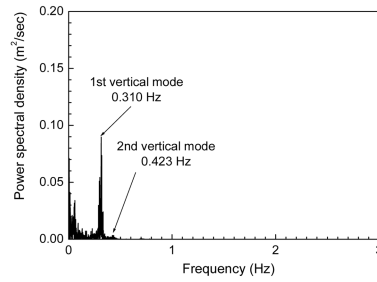
Cable	Girder maximum amplitude (m)	Cable maximum amplitude (m)	
		Parametric and forced vibration	Forced vibration
C12	0.0766	0.2427	0.2512
C32	0.0615	0.3613	0.2219

Table 4 Maximum responses of cables C19 and C39

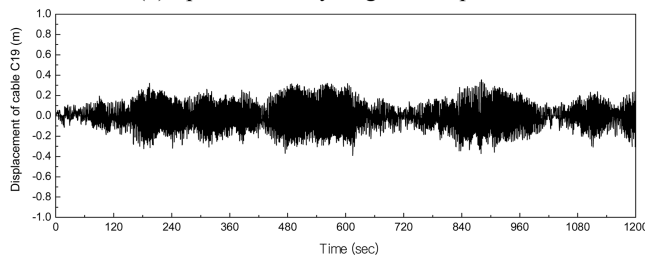
Cable	Girder maximum amplitude (m)	Cable maximum amplitude (m)	
		Parametric and forced vibration	Forced vibration
C19	0.2155	0.3913	0.2698
C39	0.1922	0.5469	0.2600



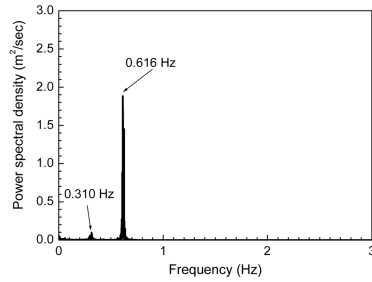
(a) Girder response



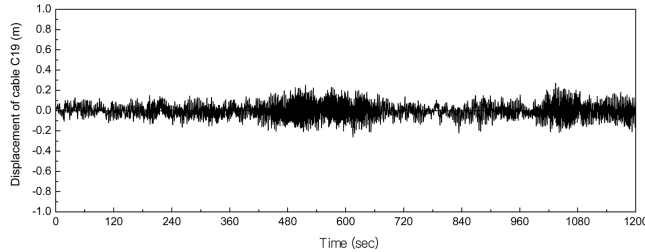
(b) Spectral density of girder response



(c) Cable C19 response



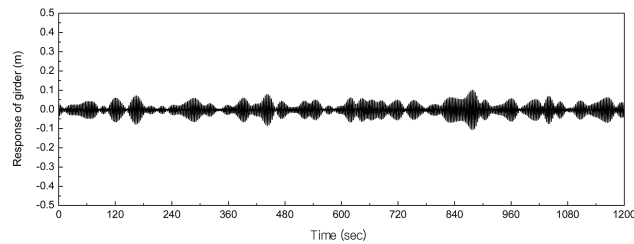
(d) Spectral density of cable C19 response



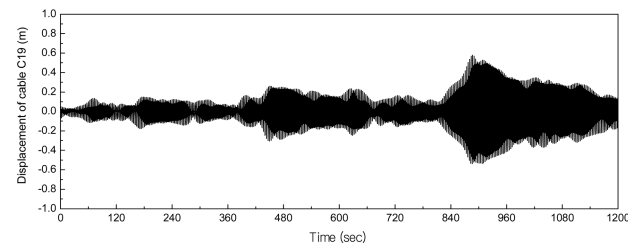
(e) Cable response under forced vibration

Fig. 11 Response of the girder and cable C19 ( $U = 30 \text{ m/s}$ ,  $h_c = 0.001$ )

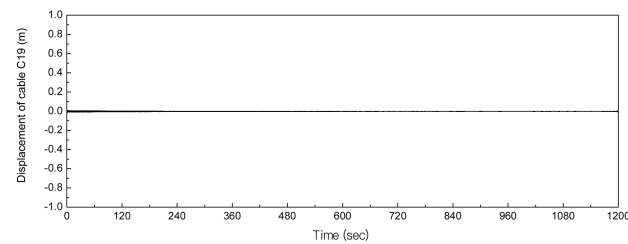
vibrations. This is because the maximum responses under combined parametric and forced vibrations are twice those of the maximum responses under forced vibration. The vibration may be either the parametric vibration in the principle unstable region or the second super-harmonic resonance, as shown in Table 2. From the spectra of the girder and cable C19, shown in Fig. 11, the most predominant frequency of response of the girder is about 0.310 Hz, while that of cable C12 is close to 0.616 Hz. It may be concluded that the second super-harmonic resonance occurs in cable C19 because the ratio of the dominant frequency of the girder to that of C12 is approximately 0.5. In order to explore this aspect, a numerical filter based upon Fourier transformation is used to keep



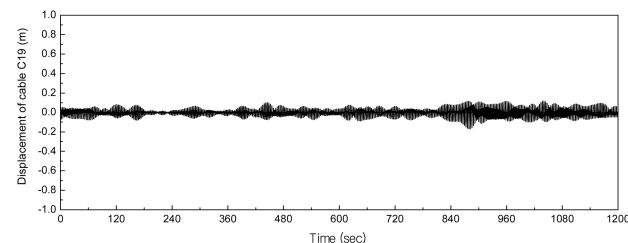
(a) Girder response in 0.280~0.340Hz region



(b) Cable response in 0.280~0.340Hz region



(c) Cable response in 1.024~1.224Hz region



(d) Cable response under forced vibration in 0.280~0.340Hz region

Fig. 12 Response of the girder and cable C19 using filter ( $U = 30$  m/s,  $h_c = 0.001$ )

the component of the response within the predicted frequency domain and to remove those outside the predicted frequency domain. As can be seen in Fig. 8, the frequency at which second super-harmonic resonance may be generated in cable C19 is about 0.310 Hz, and the frequency in which parametric vibration in the principal unstable region may be generated is 1.124 Hz. Therefore, the evaluated region is about 10% smaller than the original region and is behind those frequencies. In other words, the evaluated region of the response of the girder is within  $0.310(1\pm 10\%) \text{ Hz} \approx 0.280\sim 0.340 \text{ Hz}$  and  $1.124(1\pm 10\%) \text{ Hz} \approx 1.024\sim 1.224 \text{ Hz}$ , respectively.

Fig. 12 shows that the responses of the girder and cable C12 are in the range of 0.280~0.340 Hz and 1.024~1.224 Hz. The response of cable C19 under parametric and forced vibrations in the range of 0.280~0.340 Hz (Fig. 12(b)) is greater than the component of the response in the range of 1.024~1.224 Hz, but is greater than that generated by forced vibration (Fig. 12(d)).

Therefore, it can be confirmed that the second super-harmonic resonance occurs in cables C19 and C39.

The parametric vibrations in the principal unstable regions of the cables are difficult to be exhibited since, depending upon the magnitude of the exciting force, a certain amount of time is needed to reach the maximum amplitude in this region (Wu *et al.* 2001, Wu *et al.* 2003).

### 5.3 Damping effect

In the present analysis, the damping constants  $h_c$  of the cables are assumed to be 0.001. In fact, this bridge use high-damping rubber dampers to counteract wind-induced vibrations in the cables. Therefore, the maximum damping constant  $h_c$  of the cables is 0.004-0.005. In this paper, the phoneme of local cable vibration is not changed even the cable damping is changed a little. In order to understand the effect of cable damping, the simple method changing the damping constant of cable is used. The relationship between the maximum responses of the cables and the damping constant are shown in Fig. 13.

For cables C12, C19, C32, and C39, the maximum amplitudes decrease as the damping constant increases. Therefore, a damping constant of 0.004-0.005 is adequate for the cables on this bridge under wind gust of  $U=30 \text{ m/s}$ . This also confirms that the damper is effective for reducing local vibrations in the cables.

### 5.4 Influence of turbulent wind speed

The above results are obtained for a wind velocity of  $U=30 \text{ m/s}$ , which is less than the design wind speed ( $U=52 \text{ m/s}$ ). Fig. 14 illustrates the maximum responses of the girder and cables when the wind speed is blowing at a speed of  $U=52 \text{ m/s}$ . Under these conditions, local cable vibrations have the same properties. Vibrations at higher frequencies do not appear in the girder even when the wind speed is bellowing at  $U=52 \text{ m/s}$ .

## 6. Conclusions

This study investigates the local vibrations in the stay cables of an actual cable-stayed bridge under wind gusts. The study includes the global vibration and local vibrations analyzed using the time-domain approach. The local cables vibrations take into account not only forced vibrations but

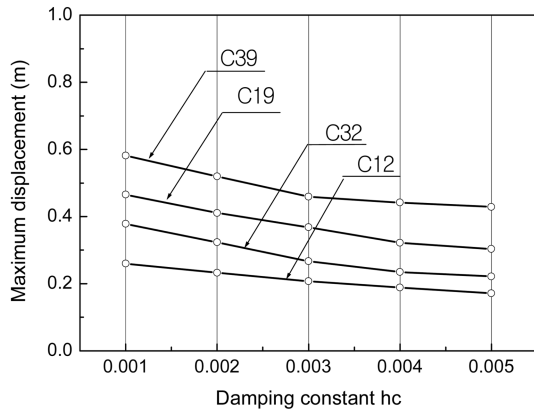


Fig. 13 Effect of damping on responses of cables

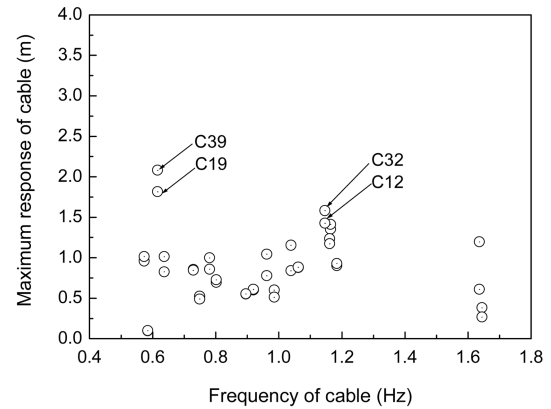


Fig. 14 Maximum responses of the girder and the cables ( $U = 52$  m/s,  $h_c = 0.001$ )

also parametric vibrations.

The results of numerical analysis using an existing cable-stayed bridge reveal a significant difference between the forced vibration and the combined parametric and forced vibrations. Among environmental loadings and service loadings, wind loading has a much greater effect than traffic loading and leads to large-amplitude vibrations in the girder and towers. Compared to the duration of an earthquake, the total time of wind loading is considerably longer. For these reasons, local vibrations in cables are more likely to occur in windy conditions than as a result of a moving vehicle or an earthquake.

Turbulent wind produces parametric vibrations in the second unstable region of cables. Parametric vibration induces greater amplitudes than forced vibration. Second super-harmonic resonance occurs in the bottom cables of this bridge. The half of the frequencies of the bottom cables is small and prone to the first mode of global vibration, since the initial force of the bottom cables are relatively small and the frequency of the first global mode is small in a steel cable-stayed bridge.

The damping adopted to counteract wind-induced vibrations in the cables effectively reduces local nonlinear vibration in the cables.

For this steel bridge, the local cable vibration can be separated from the deck-tower-cable global vibration, and the local cable vibration is discussed based on the global vibration. This study does not consider the interaction between the bridge (deck/tower) and the stay cables since the laboratory did not have the FE model needed to evaluate parametric vibrations of the cables. An appropriate FE model for cables is now being formulated.

The next subject for study is a gust response analysis of cable-stayed bridges that includes the parametric vibrations and ellipse vibrations of the stay cables. Another subject is using this model to evaluate the questionable problem: whether the in-plane cable model can be used to three-dimensional cable-stayed vibration under wind gust; how much the difference between in-plane cable model and the coupled in-plane and out-of-plane model is.

## Acknowledgements

The research reported herein is the Project 50808047 supported by National Natural Science

Foundation of China. It is also supported by Program for New Century Excellent Talents in Fujian Province University (NCETFJ 2007).

## References

- Abdel-Ghaffar, A.M. and Khalifa, M.A. (1991), "Importance of cable vibration in dynamics of cable-stayed bridges", *J. Eng. Mech.*, ASCE, **117**, 2571-2589.
- Au, F.T.K., Cheng, Y.S., Cheung, Y.K. and Zheng, D.Y. (2001), "On the determination of natural frequencies and mode shapes of cable-stayed bridges", *Appl. Math. Model.*, **25**, 1099-1115.
- Boonyapinyo, V., Miyata T. and Yamada, H. (1999), "Advanced aerodynamic analysis of suspension bridges by state-space approach", *J. Struct. Eng.*, ASCE, **125**, 1357-1366.
- Caetano, E., Cunha, A. and Taylor, C. (2000), "Investigation of dynamic cable-deck interaction in a physical model of a cable-stayed bridge: Part I: modal analysis", *Earthq. Eng. Struct. Dynam.*, **29**, 481-498.
- Caetano, E., Cunha, A. and Taylor, C. (2000), "Investigation of dynamic cable-deck interaction in a physical model of a cable-stayed bridge: Part II: seismic response", *Earthq. Eng. Struct. Dynam.*, **29**, 499-521.
- Chen, X., Matsumoto, M. and Kareem, A. (2000), "Time domain flutter and buffeting response analysis of bridges", *J. Eng. Mech.*, ASCE, **126**, 7-16.
- Davenport, A.G. (1961), "The spectrum of horizontal gustiness near the ground in high winds", *Quarterly J. Royal Meteorological Soc.*, **87**, 194-221.
- Ding, Q., Lee P.K.K. and Lo, S.H. (2000), "Time domain buffeting analysis of suspension bridges subjected to turbulent wind with effective attack angle", *J. Sound Vib.*, **233**, 311-327.
- Fujino, Y., Warnitchai, P. and Pacheco, B.M. (1993), "An experimental and analytical study of autoparametric resonance in a 3 DOF model of cable-stayed-beam", *Nonlinear Dynam.*, **4**, 111-138.
- Fujino, Y., and Kimura, K. (1997), "Cables and cable vibration in cable-supported bridges", *Proceedings of International Seminar on Cable Dynamics, Technical Committee on Cable Structures and Wind*, Japan Association for Wind Engineering, 1-11.
- Gill, P.E. and Murray, W. (1972), "Quasi-newton methods for unconstrained minimization", *J. Inst. Math. Appl.*, **9**, 91-108.
- Gimsing, N.J. (1997), *Cable Supported Bridges*, John Wiley and Sons Ltd.
- Iannizzi, A. and Spinell, P. (1987), "Artificial wind generation and structural response", *J. Struct. Eng.*, ASCE, **113**, 2382-2398.
- Irvine, H.M. (1981), *Cable Structures*, The Massachusetts Institute of Technology Press, Cambridge, MA.
- Iwatani, Y. (1982), "Simulation of multidimensional wind fluctuations having any arbitrary power spectra and cross spectra", *J. Wind Eng.*, **11**, 5-18 (in Japanese).
- Jain, A., Jones, N.P. and Scanlan, R.H. (1996), "Coupled flutter and buffeting analysis of long-span bridges", *J. Struct. Eng.*, ASCE, **122**, 716-725.
- Lilien, J.L. and Pinto Da Costa, A. (1994), "Vibration amplitudes caused by parametric excitation on cable stayed structures", *J. Sound Vib.*, **174**, 69-90.
- Panofsky, H.A. and Dutton, J.A. (1984), *Atmospheric Turbulence: Models and Methods for Engineering Applications*, Wiley-Interscience, New York.
- Pinto da Costa, A., Martins, J.A.C., Branco, F. and Lilien, J.L. (1996), "Oscillations of bridge stay cables induced by periodic motions of deck and/or towers", *J. Eng. Mech.*, ASCE, **122**, 613-622.
- Rogar, K. (1977), "Airplane math modeling methods for active control design", *AGARD-CP-228, Advisory Group for Aerodynamic Research and Development, Structural Aspects of Active Control*, Washington, D.C., 4-1-4-11.
- Scanlan, R.H. (1978), "The action of flexible bridges under wind, I: Flutter theory", *J. Sound Vib.*, **60**, 187-199.
- Scanlan, R.H. (1978), "The action of flexible bridges under wind, II: Buffeting theory", *J. Sound Vib.*, **60**, 201-211.
- Scanlan, R.H. (1988), "On flutter and buffeting mechanisms in long-span bridges", *Probabilist. Eng. Mech.*, **3**, 22-27.

- Scanlan, R.H. and Jones, N.P. (1990), "Aeroelastic analysis of cable-stayed bridges", *J. Struct. Eng.*, ASCE, **116**, 279-297.
- Simiu, E. and Scanlan, R.H. (1996), *Wind Effects on Structures*, Wiley, New York.
- Sun, D.K., Xu, Y.L., Ko, J.M. and Lin, J.H. (1999), "Fully coupled buffeting analysis of long-span cable-supported bridges: Formulation", *J. Sound Vib.*, **228**, 569-588.
- Takahashi, K. (1991), "Dynamic stability of cables subjected to an axial periodic load", *J. Sound Vib.*, **144**, 323-330.
- Tuladhar, R., Dilger, W.H. and Elbadry, M.M. (1995), "Influence of cable vibration on seismic response of cable-stayed bridges", *Can. J. Civil Eng.*, **22**, 1001-1020.
- Uhrig, R. (1993), "On kinetic response of cables of cable-stayed bridges due to combined parametric and forced excitation", *J. Sound Vib.*, **165**, 185-192.
- Warnitchai, P., Fujino, Y. and Susumpow, T. (1995), "A non-linear dynamic model for cables and its application to cable-structure system", *J. Sound Vib.*, **187**, 695-712.
- Wilde, K., Fujino, Y. and Masukawa, J. (1996), "Time domain modeling of bridge deck flutter", *J. Struct. Mech. Earthq. Eng.*, JSCE, **543**, 19-30.
- Wu, Q., Takahashi K. and Chen, B. (2006), "Using cable finite elements to analyze parametric vibrations of stay cables in cable-stayed bridges", *Struct. Eng. Mech.*, **23**(6), 691-711.
- Wu, Q., Takahashi, K., Okabayashi, T. and Nakamura, S. (2001), "Response characteristics on local vibrations of stay cables in an existing cable-stayed bridge", *Fourth International Symposium on Cable Dynamics*, Montreal, Canada, 101-108.
- Wu, Q., Takahashi, K., Okabayashi, T. and Nakamura, S. (2003), "Response characteristics of local vibrations in stay cables on an existing cable-stayed bridge", *J. Sound Vib.*, **261**, 403-420.
- Xu, Y.L., Sun, D.K., Ko, J.M. and Lin, J.H. (2000), "Fully coupled buffeting analysis of Tsing Ma suspension bridge", *J. Wind Eng. Ind. Aerod.*, **85**, 97-117.
- Yoshimura, T., Inoye, A., Kaji, K. and Savage M. (1989), "A study on the aerodynamic stability of the Aratsu Bridge", *Proceedings of Canada-Japan Workshop on Bridge Aerodynamics*, National Research Council of Canada, Ottawa, Canada, 141-50.
- Zhu L.D. and Xu Y.L. (2005), "Buffeting response of long-span cable-supported bridges under skew winds. Part 1: Theory", *J. Sound Vib.*, **281**, 647-673.